Accepted for Publication in *Polymer* (2025)

Tuning Gas Separation Performance of Polyimide Membranes with Macrocyclic Crown Ether Units

Yiwei Su[§], Andrew Seeger[§], Ruilan Guo*

Department of Chemical and Biomolecular Engineering, University of Notre Dame, Notre Dame, IN, 46556, USA

*Corresponding author: rguo@nd.edu
[§] Equal contribution

Abstract: Membrane-based gas separation is an energy-efficient alternative to conventional thermally-driven separation processes. However, polymer membranes face the permeability-selectivity trade-off challenge, which stems from the broad size distribution of free volume voids. This study reports a molecular design strategy to address this challenge through incorporating macrocyclic crown ether (CE) moieties into the backbone of Matrimid® polyimide, a commercial gas separation membrane. A series of CE-containing Matrimid®-like copolyimides were synthesized with systematically varied CE molar contents ranging from 3-20%. These copolyimides formed ductile, defect-free thin films suitable for membrane fabrication. Gas permeation tests revealed a non-monotonic relationship between permeability/selectivity and CE content. Notably, the copolyimide with only 5% CE demonstrated a 61% increase in CO_2/CH_4 selectivity and a 13% increase in CO_2 permeability relative to pristine Matrimid®. Higher CE contents did not yield further performance improvements, which is likely due to the competing effects of chain packing disruption and π–π interactions among CE moieties at high content. This hypothesis was supported by wide-angle X-ray scattering (WAXS) analysis, density measurements, and fractional free volume calculations. These findings highlight the potential of macrocyclic crown ether incorporation strategies in fine tuning the microstructure of commercial polyimide gas separation membranes to surpass the traditional permeability-selectivity trade-off.

Keywords: Crown ether, polyimide, free volume, CO_2 separation

1. INTRODUCTION

Chemical separations are fundamental to numerous industrial processes, underpinning sectors such as energy production (e.g., natural gas purification, hydrogen separation), environmental management (e.g., water treatment, carbon capture), and chemical manufacturing. Traditionally, these separations have relied heavily on thermally-driven separation techniques, such as distillation, which are energy intensive and account for approximately 10-15% of global energy consumption[1–3]. Membrane-based separation technologies have emerged as energy-efficient alternatives, offering lower operational costs and reduced environmental impact[4–7].

Among various membrane materials for separation applications, polymer membranes are arguably the most widely used membrane materials due to relatively low cost and excellent processability allowing for feasible fabrication into various membrane modules such as hollow fibers or flat sheet membranes[8–11]. Polymer membranes, particularly those made from aromatic polyimides and polysulfones, are widely used in industrial applications such as natural gas purification and air separation [5,12].

However, polymeric gas separation membranes often face a trade-off between permeability and selectivity, a relationship encapsulated by the well-known Robeson upper bound limits for various gas pairs[13,14]. For polymer gas separation membranes following the solution-diffusion mechanism, gas separation performance is governed by the polymer free volume architecture (i.e., gas transport pathways) and the affinity of between gas molecules and polymer membrane. Ideally, a high-performance polymer membrane should have large fractional free volume for high permeability, well-define size distribution of free volume voids for high selectivity, as well as strong affinity toward select gas molecules[15]. Recent development of high-free-volume polymers, such as ladder-like polymers, has pushed these permeability-selectivity boundaries[16–

18]. While highly attractive separation performances were demonstrated, their complex synthesis, scalability issues, and more importantly, their susceptibility to physical aging due to free volume collapse greatly limit their practical application[19,20]. In this regard, incorporation of moieties that possess intrinsic, non-collapsible, and well-defined molecular cavities hold great promise to produce high performance size-sieving separation membranes.

A promising strategy is to incorporate macrocyclic structure units, such as crown ether, into polymer backbone structures, which can introduce well-defined, configuration-based free volume cavities enabling strong size-sieving effect. Pedersen first synthesized crown ethers and analyzed their complexes with metal salts in 1967[21]. Since then, crown ethers have been studied for various applications due to their unique cyclic structure and host-guest interaction. Recently, there are increasing interests in incorporating crown ether into polyimide membranes to improve the gas separation performance. For instance, Wu. et al. prepared a series of copolyimides containing dibenzo-18-crown-6 and -CF_3 groups, which showed increasing fractional free volume (FFV) and fractional accessible volume (FAV) leading to enhanced CO_2 permeability and approaching the 2008 upper bound for CO_2/CH_4 separation with 30 mol% crown ether content[22,23]. Zhang et al. reported incorporating dibenzo-21-crown-7 in copolyimides, which hit the 2008 CO_2/CH_4 upper bound[24]. Kim et al. studied copolyimides containing dibenzo-18-crown-6 and polydimethylsiloxane (PDMS) with enhanced CO_2 selectivity, where the rigid structure of crown ethers enhances CO_2 affinity, while PDMS increases permeability at relatively low content (5%)[25]. A study demonstrated that a carbon molecular sieve membrane derived from a crown ether-containing copolyimide precursor exhibited high CO_2 permeability and selectivity, surpassing the 2015 upper bound for H_2 separation and the 2019 upper bound for CO_2 separation[26]. These studies highlight the potential of crown ether incorporation in polyimide

membranes to enhance gas separation performance. However, these studies focus on polyimide structures containing bulky CF_3 groups and incorporate relatively high crown ether content (>10%), which have higher cost and may potentially have environmental concerns. In this work, the incorporation of 18-crown-6 moieties into commercial Matrimid®-like polyimides is investigated to systematically examine the effect of crown ether on gas transport while establishing fundamental structure-property relationships to guide the future design of novel gas separation membrane materials containing macrocyclic moieties. A series of Matrimid®-like copolyimides containing crown ether in systematically varied molar content, ranging from 5% to 20%, were developed via polycondensation of Matrimid® polyimide using an 18-crown-6-based diamine as a comonomer. The effects of crown ether content on polymer chain packing and gas transport properties were comprehensively examined. Gas permeability and selectivity of these crown ether-containing copolyimides showed non-monotonic dependence on the crown ether content. This result, in addition to analyses of copolyimide chain packing, suggest that there is likely an optimal range of crown ether content to balance the effect of disrupted chain packing due to the bulkiness of crown ether and the effect of stacking of crown ether moieties.

2. EXPERIMENTAL

2.1. Materials

3, 3′, 4, 4′-benzophenone tetracarboxylic dianhydride (BTDA, 97+%) from Alfa Aesar was dried at 160 °C in vacuum oven overnight before use. 4′, 5-/6-, diamino-1,3,3-trimethyl-1-phenylindan (DAPI) was received from Dokitton, Switzerland and dried at 40 °C in vacuum oven overnight before use. Chloroform was purchased from VWR and used as received. 200 proof Ethanol was purchased from Decon Labs and used as received. Hydrazine monohydrate was purchased from Alfa Aesar and used as received. Dibenzo-18-crown-6 (DB18C6) was purchased from TCI

chemicals and used as received. Nitric acid (70%), Glacial acetic acid, methanol, and palladium on active charcoal (Pd/C) were purchased from Sigma-Aldrich and used as received. Anhydrous dimethyl sulfoxide (DMSO), dimethylacetamide (DMAc), and toluene were purchased from EMD Millipore and used as received.

2.2. Synthesis of di(nitrobenzo)-18-crown-6 (DNB18C6)

Di(nitrobenzo)-18-crown-6 (DNB18C6) was synthesized following previously reported methods[27,28] with slight improvements as shown in **Scheme 1**. A typical synthesis of DNB18C6 is as follows: A 500 ml round-bottom flask equipped with a magnetic stirrer and a condenser was charged with 5.00 g (13.9 mmol) of dibenzo-18-crown-6, 70 ml glacial acetic acid, and 135 ml chloroform. The solution was stirred for 10 min at room temperature to dissolve the DB18C6. After a clear solution was formed, a mixture of 15 ml nitric acid and 30 ml acetic acid was then added to the flask dropwise over 20 min. After stirring at room temperature for 1 h, the temperature was brought up to 60 °C to react for another 6 h. Then the solution was cooled to room temperature, poured into 1200 ml deionized (DI) water, and stirred overnight. A yellow precipitate was collected and washed with water three times, dried at 100 °C in a vacuum oven for 12 h to obtain the final product DNB18C6 as a light-yellow powder in 94.4% yield and high purity as evidenced by ^{1}H NMR (**Fig. 1**).

Scheme 1. Synthesis of diamine monomer DAB18C6 containing 18-crown-6 moieties

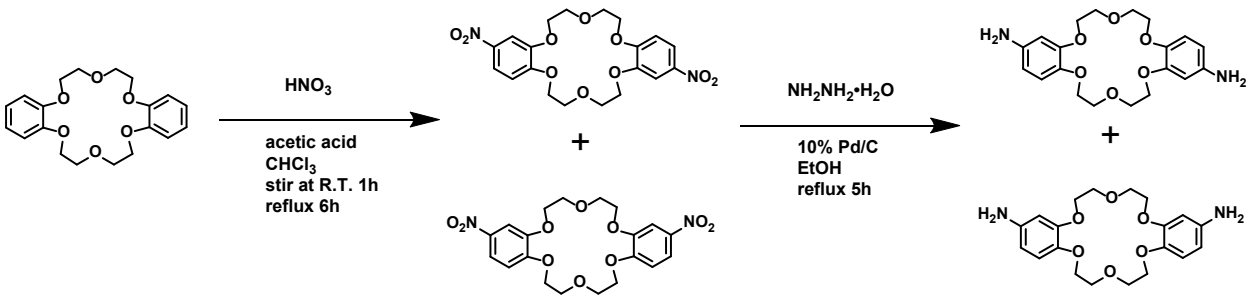

2.3. Synthesis of di(aminobenzo)-18-crown-6 (DAB18C6)

Di(aminobenzo)-18-crown-6 (DAB18C6) monomer was synthesized following previously reported method[27,28] with some improvements. A typical synthesis of DAB18C6 is as follows: A 500 ml round-bottom flask equipped with a magnetic stirrer, a condenser, and a nitrogen inlet adaptor was charged with 5.80 g (12.8 mmol) DNB18C6, 1.00 g Pd/C, and 250 ml ethanol under nitrogen atmosphere. The mixture was heated up to 80 °C to dissolve the DNB18C6 before 40 ml of hydrazine monohydrate was added dropwise over 20 min. The mixture was allowed to reflux for 5 h, then hot-filtered to remove the Pd/C. The clear filtrate solution was treated with rotary evaporation till about half of the solvent was removed. After cooling down, a white powder precipitation was observed, filtered, washed with water three times, and dried at 100 °C in a vacuum oven for 12 h to obtain the final product as a white powder with a yield of 72.5% and high purity as confirmed by ^{1}H NMR (**Fig. 1**).

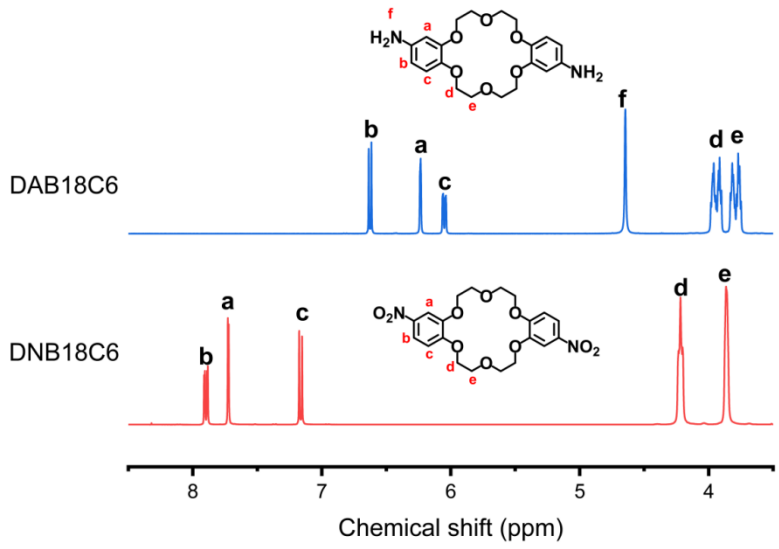

Fig. 1. ^{1}H NMR spectra of DNB18C6 (the nitro intermediate) and DAB18C6 (the final diamine monomer)

2.4. Synthesis of random copolyimides with controlled crown ether content

A series of Matrimid-DAB18C6 random copolyimides with different crown ether content were synthesized via condensation polymerization of BTDA, DAB18C6, and DAPI using isoquinoline as catalyst and toluene as azeotropic solvent to remove water (**Scheme 2**). The resulting copolyimides are named as MM-DAB18C6(x%), where x% refers to the molar percentage of the repeating units containing 18-crown-6 moieties. A sample polymerization of MM-DAB18C6(20%) is as follows: A 150 ml round-bottom 3-neck flask equipped with a mechanical stirrer, a nitrogen inlet adaptor, a Dean-Stark trap, and a condenser was charged with 0.60 g DAPI (2.25 mmol), 0.22 g DAB18C6 (0.56 mmol), and 4 ml of NMP. After 15 min stirring at room temperature to form a clear solution, 0.91 g BTDA (2.81 mmol) and 5 ml NMP were added to the flask, and the solution was allowed to react overnight at room temperature, under nitrogen atmosphere, to form a viscous poly(amic acid) solution. To thermally imidize the poly(amic acid) intermediate, 3 ml of toluene and 1.5 ml of isoquinoline were added to the flask, and the temperature was brought to 160 °C. The Dean-Stark trap was filled with toluene to let toluene reflux inside the flask to bring out water in the system during imidization. The solution was allowed to react for 6 h to form a viscous polyimide solution. The resulting solution was precipitated in 600 ml methanol and stirred overnight, then filtered, dried in vacuum oven overnight at 100 °C. The collected solids were redissolved in NMP and reprecipitated in methanol to completely wash out the residual isoquinoline. After filtration and drying in vacuum oven overnight at 100 °C the final product MM-DAB18C6(20%) was obtained as a brown powder with a yield of 95%.

Scheme 2. Synthesis of the Matrimid®-like copolyimides containing DAB18C6 moieties

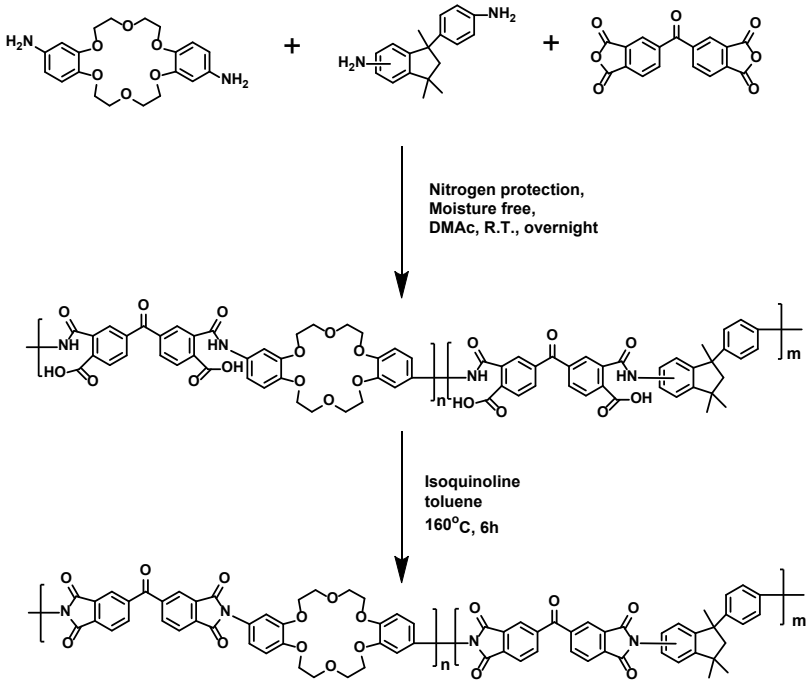

2.5. Thin film preparation

Thin films of all the synthesized MM-DAB18C6 copolymers were prepared via solution-casting method. A typical process is as follows: 0.135 g of the polymer was dissolved in 3 ml DMAc to form a 4.5% w/v solution. After filtered through a 1 μm syringe filter, the filtrate was cast onto a leveled, clean glass plate and dried in vacuum oven at 80 °C for 24 h or 48 h to form a flexible, transparent thin film with thickness of about 30-40 μm. The film was then separated from the glass plate, soaked in methanol overnight, and dried in vacuum oven at 100 °C for 12 h. The final thin films were stored in a cool, dry place at room temperature until further use.

2.6. Polymer and film characterizations

Proton nuclear magnetic resonance (^{1}H NMR) spectra were recorded on a Bruker AVANCE III HD 400 Nanobay spectrometer with DMSO-d_6 as the solvent. Fourier-transform infrared (FTIR) spectra were recorded using a JASCO FT-IR 6300 spectrometer at 4 cm^{-1} resolution with 64 scans.

Differential scanning calorimetry (DSC) was performed using a DSC Q2000 under 50 ml/min of N_2 flow. The samples were first heated from 30 °C to 300 °C at 10 °C/min to remove thermal history before cooling to 100 °C and ramping up to 350 °C. DSC profiles were reported based on second heating cycle. Thermogravimetric analysis (TGA) was performed on film samples using a TGA Q500 under 50 ml/min of N_2 flow to ensure complete solvent removal, where film samples were heated to 600 °C from room temperature at a rate of 10 °C/min.

Wide angle x-ray scattering (WAXS) was performed using a Malvern Aeris benchtop X-ray diffractometer. The instrument was set to reflection mode at 40 mA and 40 kV using a Cu Kα radiation source with a wavelength of 1.54 Å.

Fractional free volume (FFV) of polymer thin films was calculated using the following equation,

$$FFV = \frac{V - V_{oc}}{V}$$

where V (cm^3g^{-1}) is the specific volume, determined through buoyancy measurements, and V_{oc} (cm^3g^{-1}) is the occupied volume calculated by: $V_{oc} = 1.3 \times V_{vw}$ with V_{vw} being the van der Waals volume determined through Bondi's group contribution method[29,30], and 1.3 as an empirically determined packing factor.

2.7. Gas permeation measurement

To test pure-gas permeation, a fixed-volume variable-pressure gas cell system was used[31]. Film samples were loaded into the cell, degassed for at least 12 h, and then tested at 35 °C with H_2, CH_4, N_2, O_2, and CO_2. For each gas, five pressures, in 50 psi intervals, between 30 and 230 psi were tested to ensure no defects were present in the samples. The permeability at each pressure was calculated using the following equation:

$$P = 10^{10} \frac{V_d l}{p_{up} RTA} \left[\left(\frac{dp}{dt} \right)_{ss} - \left(\frac{dp}{dt} \right)_{leak} \right]$$

Where V_d is the downstream volume of the cell in cm^3, l is the measured thickness of the film in cm, p_{up} is the gauge pressure of the upstream in cm Hg, A is the exposed membrane area in cm^2, R is the gas constant (0.278 cm^3 cm Hg/cm^3(STP)*K), T is the test temperature in K, $(dp/dt)_{ss}$ and $(dp/dt)_{leak}$ are the rate of pressure increase (cm Hg/s) in the downstream and the leak rate, respectively.

Fundamental transport properties are analyzed in terms of diffusivity coefficient (D, in cm^2/s) and solubility coefficient (S, in cm^3(STP)/(cm^3 cmHg)). Diffusivity coefficient, D, was determined using the lag time method as $D = \frac{l^2}{6\theta}$, where l is the film thickness, and θ is the lag-time[31,32]. The solution-diffusion model, $P = D \times S$, is then utilized to find the solubility coefficient.

Mixed-gas permeation measurements of the CO_2/CH_4 gas pair were performed at 50 °C in a constant pressure/variable volume gas cell[31]. The CO_2:CH_4 mixture was fed into the system at a 20:80 molar ratio at a pressure of 300 psi needed to achieve a reading. The stage-cut was under 0.5% with a feed flow rate of 200cm^3(STP)min^{-1}. A 3000 Micro GC, Infinicon with a thermal conductivity detector was used to measure the permeate compositions. The permeability of a gas in the binary mixed-gas system was calculated by:

$$P_A = \frac{x_A S l}{x_{sweep}(P_{2A} - P_{1A})}$$

where x_A and x_{sweep} are the mole fractions of component A and the sweep gas, respectively, S is the flowrate of sweep gas, l is the thickness of the film, P_{2A} and P_{1A} are the partial pressures of gas A in the feed and permeate, respectively.

3. RESULTS AND DISCUSSION

3.1. Synthesis and characterization of 18-crown-6-based MM-DAB18C6 copolyimides

A series of MM-DAB18C6 random copolymers with controlled molar fraction of crown ether ranging from 3% to 20% were synthesized as described in section 2.4. High molecular weight polymers were obtained in all copolymer compositions as evidenced by fibrous precipitation and the formation of robust ductile thin films of all the copolyimides (**Fig. S1**). The fully imidized structures of copolyimides and the molar content of crown ether rings are confirmed via ^{1}H NMR spectra as shown in **Fig. 2**. As shown, the intensity of the characteristic peaks of the crown ether ring (e.g., peaks m and n) increases with the increase of crown ether content. The actual molar fractions of the crown ether are calculated using ^{1}H NMR analysis by taking the integration ratio between peak m and peak j, which are the characteristic peaks of DAB18C6 and DAPI, respectively. The actual crown ether molar contents match well with the target contents, indicating successful polymerizations with well-controlled crown ether content.

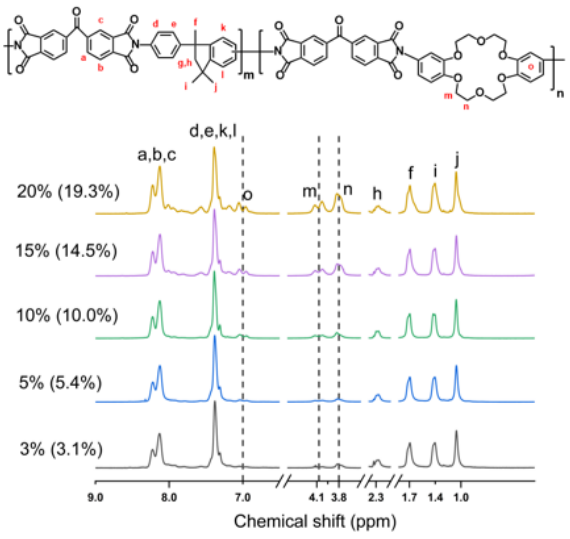

Fig. 2. ^{1}H NMR spectra of MM-DAB18C6 copolyimides with controlled crown ether content. The percentage values in parentheses are the actual crown ether molar contents determined from ^{1}H NMR analysis comparing peak intensity of DAB18C6 (peak m) and DAPI (peak j) moieties.

The FTIR results (**Fig. S2**) also confirm the fully imidized structure by the presence of C=O asymmetrical vibration band of the imide moieties at 1783 cm^{-1} and the absence of C=O bands of the amic acid intermediate. With the increase of crown ether content, the intensity of the characteristic bands of DAB18C6 increases, including the skeletal stretching of aromatic rings at 1505 cm^{-1}, the C-O-C bond asymmetric stretching vibration at 1255 cm^{-1} and symmetric stretching vibration at 1125 cm^{-1}.

Thermal properties of MM-DAB18C6 copolymers s were analyzed by TGA and DSC to determine the glass transition temperature (T_g) and the decomposition temperature ($T_{d,5\%}$). As shown in **Fig. 3a**, the T_g values of MM-DAB18C6 series are in the range between 288 °C and 309°C, depending on the crown ether content. The overall high T_g values indicate highly rigid backbone of the synthesized copolyimides. With increasing crown ether content, the T_g of the copolyimides generally decreases due to the presence of more flexible C-O-C bond in the crown ether moieties. However, when the crown ether content exceeds 10 mol%, the changes in T_g become minimal. This is likely caused by the enhanced π- π stacking interaction between the benzene rings attached to the crown ether moieties, which rigidifies the polymer backbone and counteract the flexibility introduced by the ether linkages of crown ether. The TGA profiles (**Fig. 3b**) of the casted thin films of all the copolyimides confirm all the thin films are solvent free by applying the methanol soaking procedure in film casting. The high $T_{d,5\%}$ values (>418 °C) indicate high thermal stability of the copolyimides as expected. The slightly reduced thermal stability of the copolyimides with higher crown ether content is because the C-O-C bond has relatively lower thermal stability.

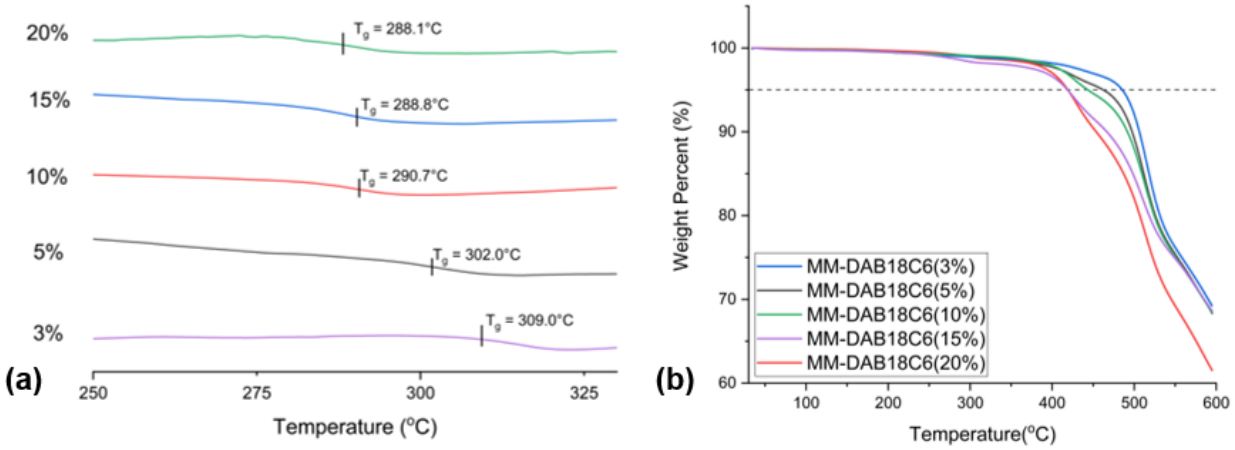

Fig. 3. (a) DSC and (b) TGA profiles of the MM-DAB18C6 copolyimides with varying 18-crown-6 molar content ranging from 3% to 20%.

3.2. Characterization of MM-DAB18C6 thin films

Polymer free volume are transient voids formed by inefficient chain packing, which provides gas transport pathways in gas separation membranes, and is a major factor for permeability and selectivity. Increasing fractional free volume usually enhances gas permeabilities, while narrowing free volume size distribution contributes to enhanced size sieving properties. Due to the unique cyclic structure of dibenzo-crown-ether, the corresponding dense polymer thin films usually show decreased fractional free volume content with increased selectivity. This has already been observed in several different studies with both experiments and simulations, and could attribute to the stacking of crown ether rings, which creates low barrier transport pathways and largely facilitates the separation toward target molecules[23,25,33,34].

The results of film density and the calculated fractional free volume (FFV) as a function of the crown ether (CE) content are tabulated in **Table 1**. Compared to pure Matrimid® polyimide with a FFV of ~13.7%[35], the incorporation of CE moieties into the polymer backbone generally led

to increases in FFV in all the copolyimides. This increasing trend in FFV with increasing CE content, however, is not monotonic, which is likely due to the competing effects between chain packing disruption by the CE macrocycles and tightened chain packing by the π-π stacking of benzene rings attached to the CE moieties For MM-DAB18C6(3%) and MM-DAB18C6(5%) films with low CE content where the π-π stacking effect is not significant, chain packing is effectively disrupted due to the introduction of relatively bulky CE macrocycles that may reduce the interaction of the charge transfer complex between the imide rings. With the increase of CE content, it is likely that the crown ether moieties might aggregate or assemble enabling strong π-π stacking of the benzene rings attached to the CE units, resulting in tightened chain packing and thus reduced FFV.

Table 1. Density, calculated fractional free volume (FFV), and *d*-spacing of MM-DAB18C6 copolyimide thin films

	Matrimid®[35]	**MM-DAB18C6 copolyimides**				
CE content	0%	3%	5%	10%	15%	20%
Density (g/cm^3)	1.252 (±0.002)	1.262 (±0.008)	1.252 (±0.010)	1.267 (±0.004)	1.266 (±0.004)	1.288 (±0.008)
Vw (cm^3/g)	288.4	289.8	290.7	293.0	295.3	297.6
FFV (%)	13.7 (±0.1)	14.7 (±0.5)	15.5 (±0.7)	14.8 (±0.3)	15.1 (±0.3)	13.9 (±0.5)

The *d*-spacing determined by WAXS provides the chain packing information in polymer thin films, where smaller *d*-spacing values indicate tighter chain packing and consequently lower FFV, which typically leads to lower gas permeability but potentially enhanced selectivity. The WAXS spectra of MM-DAB18C6 thin films (**Fig. 4**) show no sharp peaks indicating the completely amorphous nature of all the copolyimides as expected. Two broad peaks are observed to be centered around

2θ = 15.5° and 23.5°, which correspond to *d*-spacing values of around 5.7 Å and 3.8 Å, respectively, based on Bragg's law. The peak with *d*-spacing of ~5.7 Å is likely attributed to the average interchain distance of Matrimid®-like BTDA-DAPI polyimide segments, and the peak with a smaller *d*-spacing of 3.8 Å is likely related to the π-π stacking of the benzene rings attached to the crown ether moieties of BTDA-DAB18C6 segments. As a general observation, the relative intensity of the two peaks shifts with the increase of the crown ether content, where the peak with a smaller *d*-spacing of 3.8 Å becomes increasingly significant. This indicates more π-π stacking between the polymer chains in copolyimides with increased CE content, which is consistent with the decreasing trend in fractional free volume at higher CE content as discussed earlies.

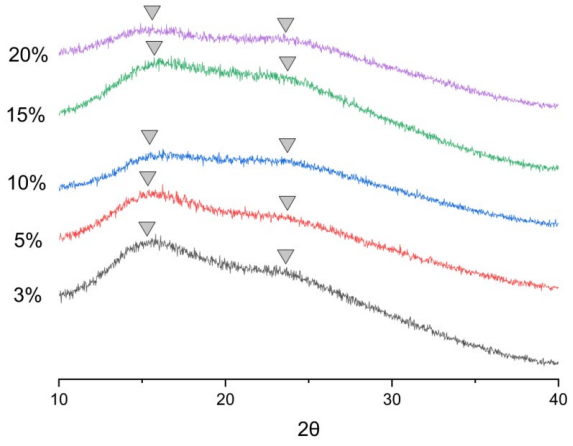

Fig. 4. WAXS profiles of MM-DAB18C6 copolyimide thin films with varying crown ether molar content.

3.3. Gas separation performance of MM-DAB18C6 copolyimide thin films

Several compositions of the MM-DAB18C6 copolymers were tested for gas permeation properties, ranging from 3 to 20 mol% incorporation of the crown ether with five different light gases at 35 °C and 30-230 psi feed pressure. The gas permeability data is plotted in **Fig. 5(a)** and the raw data is tabulated in **Table S1**. In comparison to pure Matrimid® polyimide, the gas permeabilities of MM-

DAB18C6 copolyimides decreased with the incorporation of crown ether moieties, with the exception of CO_2, which initially shows an increase in permeability until the 10% film when it falls back to the initial level of pure Matrimid®. The dependence of gas permeability on the CE content doesn't follow a simple monotonic trend and seems to be specific to different gases. Specifically, for small gases like H_2, CO_2 and O_2, their permeabilities see a slight increase with CE content up to 5%, then decrease monotonically until 20% where all gases see a slight increase. This trend is consistent with the results of FFV and chain packing discussed earlier. The increase of permeability at 20% CE content is likely due to certain alignment of the crown ether rings that leads to the formation of low-barrier transport pathways for small gases. For large gases like N_2 and CH_4, their permeabilities monotonically decrease with the CE content since permeabilities of large gases are more likely dominated by the effect of tightened chain packing due to π-π stacking.

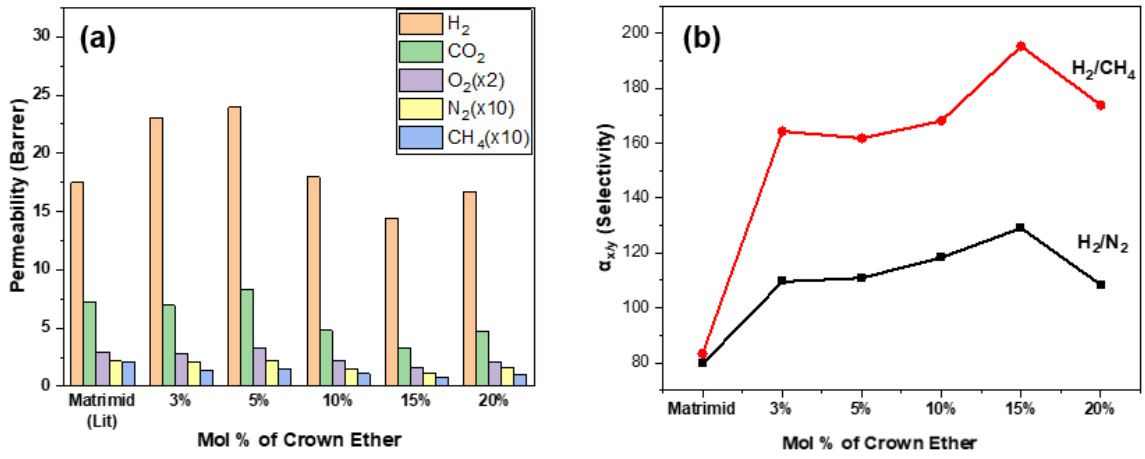

Fig. 5. (a) Pure-gas permeability and (b) idea selectivity of MM-DAB18C6 copolyimide thin films as a function of crown ether (CE) molar content ranging from 3 to 20 mol% (35 °C, 130 psi) in comparison with pure Matrimid® polyimide[36].

One of the obvious advantages from the incorporation of crown ether moieties is the selectivity increase for CO_2 containing gas pairs and H_2 separations as shown in **Fig. 5(b)**. It can be seen that even an incorporation as low as 3% CE can increase the selectivity of H_2/CH_4 by up to ~2 times that of the original Matrimid® polyimide. This effect can likely be attributed to the CO_2-philic nature of the ether groups[37] located in the crown ether ring that enhances the CO_2 permeability via solubility contribution whilst the other similarly large gases, such as N_2 and CH_4, show a decrease in permeability because they are governed more strongly by diffusivity rather than solubility. For H_2/CH_4 and H_2/N_2 separations, the much-increased selectivity is primarily dictated by size sieving wherein small H_2 is much less sensitive to the reduction of free volume due to the incorporation of CE moieties than large gases like CH_4 and N_2.

Analysis of diffusivity (D) and solubility (S) coefficients provides fundamental insights into gas transport mechanisms in polymer thin films. Diffusivity coefficients were determined using the lag time method, and solubility coefficients were calculated from permeability and diffusivity coefficient based on the solution-diffusion model, $P = D \times S$. The results are shown in **Fig. S3** and tabulated in **Table S2** as well. Diffusivity for all gases first increases until 5% incorporation whereafter it decreases or remain relatively constant as the crown ether content increases, which is consistent with the free volume decreasing as the incorporation increases as previously shown. This is likely due to the increased chain flexibility caused by having the more alkyl-like crown ether moiety, which is also demonstrated in the DSC data where the increasing CE lowered the glass transition temperature. Upon reaching the 20% CE content, however, all gases show an increase in diffusivity, which could be the result of reaching a more ideal chain packing pattern involving the alignment or assembly of the crown ether rings leading to the formation of low barrier transport pathways.

Examining solubility coefficient shows a similar trend, where, up to 15% CE content, the solubility of gases has a decreasing trend with higher CE inclusions, including CO_2 contrary to the previous assumption about ether groups likely due to the effect of reduced fractional free volume. Upon reaching 20% CE content, some solubility increases can be seen with CO_2 having a ~7% increase compared to the 15% CE content. This is an almost identical change to O_2 which shows a ~6% increase when increased from 15% to 20%. In this system, it seems that structural effects from chain packing are likely the most important factor in solubility rather than the presence of ether groups as would be expected for CO_2.

To evaluate the plasticization behavior, copolyimide thin films underwent pure gas CO_2 permeability tests under five pressures up to 230 psi, and the pressure dependence of CO_2 permeability is plotted in **Fig. 6**. At low CE content, the films show fairly consistent plasticization points at around 80 or 130 psi up until 10% CE content. When the CE content moves up to 15%, the films don't show a plasticization pressure up to 230 psi feed pressure. This change in the plasticization behavior could line up with the densification from tighter chain packing that occurs as CE content increases due to the improved intermolecular π-π interaction between the benzene rings of the crown ether moieties

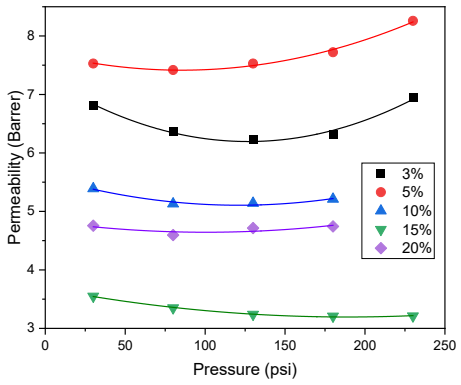

Fig. 6. Pressure dependence of CO_2 permeability for MM-DAB18C6 copolyimides with varying CE molar content.

The overall gas separation performance of the copolyimides is plotted against Robeson upper bounds for various gas pairs (**Fig. 7**) in order to compare the effect of crown ether inclusion to both commercial Matrimid® polyimide and the highest achieved performances among the copolyimide series. For all gas pairs, the selectivity increased pushing all the CE containing films closer to the 1991 upper bound. The permeability trends across composition tend to first move the low content films towards the upper bound before strong drops in permeability moves the films further towards the left side of the plot. In the CO_2/CH_4 separation, the 3 and 5% CE compositions maintain permeability while drastically increasing in selectivity showing a 44% and 58% increase, respectively. H_2 separations also saw a large increase in performance with a similar trend in the permeability of the various compositions but a sizeable increase in selectivity across all compositions. This is observable in both the H_2/N_2 separation as well as the H_2/CH_4 separation where the all CE containing films saw selectivity increases of 150% and 200%, respectively. In every separation observed the low CE content films show the best performance with the 3% and 5% CE composition films generally increasing in both selectivity and permeability, demonstrating that small incorporations of CE can have a large impact on separations.

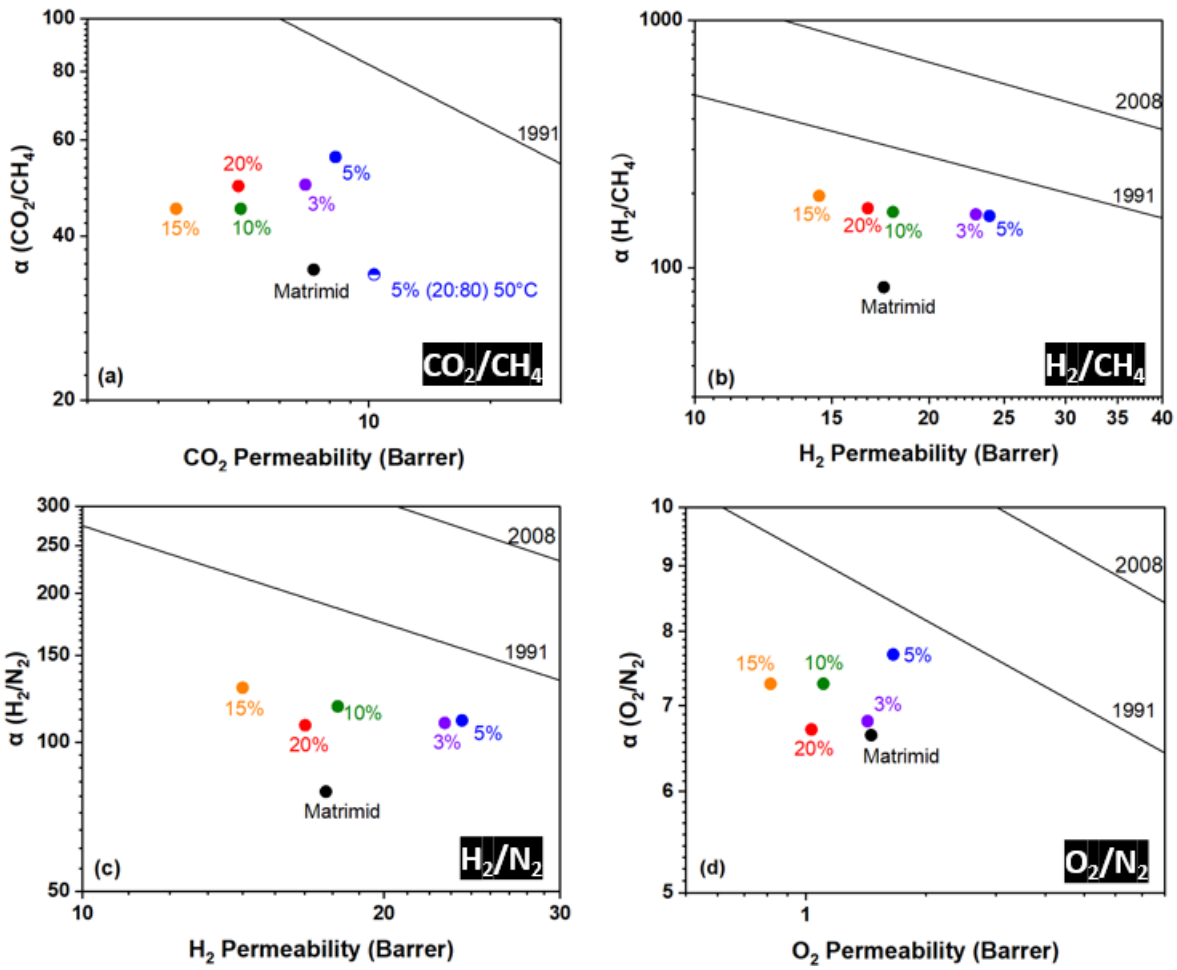

Fig. 7. Gas separation performance of MM-DAB18C6 copolyimides with varying crown ether content (3-20 mol%) benchmarked with Robeson's upper bounds for (a) CO_2/CH_4, (b) H_2/CH_4, (c) H_2/N_2, and (d) O_2/N_2. CO_2/CH_4 mixed-gas permeation data is represented in half-filled blue circle. Data of Matrimid® are from [36].

The mixed-gas separation was also tested for the CO_2/CH_4 (20:80) gas pair to assess the separation performance of the copolyimides bearing crown ether moieties under realistic conditions. Thin film of MM-DAB18C6 (5%) was chosen for the mixed-gas permeation test due to its best overall CO_2/CH_4 separation performance displayed in pure-gas permeation tests, as gauged by its smallest performance gap to the CO_2/CH_4 upper bound among all the copolyimides. Due to the very low

permeability of CH_4 at ambient conditions that barely had any signals in the GC output, the mixed-gas CO_2/CH_4 permeation measurements were conducted at 50 °C with the feed pressures of 80, 130, 230, and 300 psi, where the film showed no measurable CH_4 permeability until 300 psi. Under these conditions where the film was already beyond the plasticization point based on the pure-gas permeation tests, a visible increase of ~28% in CO_2 permeability and the selectivity loss of ~40% were expected to be observed for a plasticized film. Despite the plasticization, the film containing just 5% CE maintained selectivity comparable to the pure gas selectivity of pure Matrimid® with slightly increased permeability. This is very promising for future applications of crown ether moieties for CO_2/CH_4 separations as the performance can improved using only a miniscule amount of these macrocycle moieties.

4. CONCLUSIONS

A series of crown ether (CE)-containing Matrimid®-like copolyimides with systematically varied CE molar contents (3%, 5%, 10%, 15% and 20%) were successfully synthesized. These copolyimides formed ductile, defect-free thin films and were characterized with respect to their microstructure (chain packing and fractional free volume) and gas permeation properties. The CE-containing copolyimide films demonstrated enhanced overall gas separation performance well above that of pure Matrimid® polyimide under pure gas permeation conditions. In terms of the effect of CE content, gas permeation tests revealed a non-monotonic relationship between permeability/selectivity and CE content likely due to the competing effects of chain packing disruption and intermolecular π–π interactions among CE moieties at elevated concentrations. In particular, the copolyimide with only 5% CE demonstrated a 61% increase in CO_2/CH_4 selectivity and a 13% increase in CO_2 permeability relative to pristine Matrimid®, highlighting the potential

of macrocyclic incorporation strategies in fine tuning the microstructure of polymer gas separation membranes to overcome the traditional permeability-selectivity trade-off.

5. AUTHOR CONTRIBUTIONS

Yiwei Su: Conceptualization, methodology, validation, formal analysis, investigation, data curation, writing – original draft, writing – review & editing, visualization. ***Andrew Seeger:*** Conceptualization, methodology, validation, formal analysis, investigation, data curation, writing – original draft, writing – review & editing, visualization. ***Ruilan Guo:*** Conceptualization, Resources, writing – review & editing, supervision, project administration, funding acquisition.

6. DECLARE OF COMPETING INTEREST

The authors declare that they have no known competing financial interests or personal relationships that could have appeared to influence the work reported in this paper.

7. ACKNOWLEDGEMENTS

The authors acknowledge the financial support from the Division of Chemical Sciences, Biosciences, and Geosciences, Office of Basic Energy Sciences of the U.S. Department of Energy (DOE), under award no. DE-SC0024384. The authors thank the Center for Environmental Science and Technology (CEST) of the University of Notre Dame for the use of characterization facilities.

REFERENCES

[1] D.S. Sholl, R.P. Lively, Seven chemical separations to change the world, Nature 532 (2016) 435–437. https://doi.org/10.1038/532435a.

[2] J.L. Humphrey, G.E. Keller, Separation process technology, McGraw-Hill New York, 1997.

[3] P. Angelini, T. Armstrong, R. Counce, W. Griffith, T. LKlasson, G. Muralidharan, C. Narula, V. Sikka, G. Closset, G. Keller, others, Materials for separation technologies: Energy and emission reduction opportunities, DOE, EERE Office, Washington, DC 103 (2005).

[4] Y. Han, W.S.W. Ho, Polymeric membranes for CO2 separation and capture, J Memb Sci 628 (2021) 119244.

[5] D.F. Sanders, Z.P. Smith, R. Guo, L.M. Robeson, J.E. McGrath, D.R. Paul, B.D. Freeman, Energy-efficient polymeric gas separation membranes for a sustainable future: A review, Polymer (Guildf) 54 (2013) 4729–4761.

[6] J. Deng, Z. Huang, B.J. Sundell, D.J. Harrigan, S.A. Sharber, K. Zhang, R. Guo, M. Galizia, State of the art and prospects of chemically and thermally aggressive membrane gas separations: Insights from polymer science, Polymer (Guildf) 229 (2021) 123988.

[7] S. Luo, T. Han, C. Wang, Y. Sun, H. Zhang, R. Guo, S. Zhang, Hierarchically microporous membranes for highly energy-efficient gas separations, Industrial Chemistry & Materials 1 (2023) 376–387.

[8] K. Ghosal, B.D. Freeman, Gas separation using polymer membranes: an overview, Polym Adv Technol 5 (1994) 673–697.

[9] M. Ulbricht, Advanced functional polymer membranes, Polymer (Guildf) 47 (2006) 2217–2262.

[10] S. Kim, Y.M. Lee, High performance polymer membranes for CO2 separation, Curr Opin Chem Eng 2 (2013) 238–244.

[11] R.S.K. Valappil, N. Ghasem, M. Al-Marzouqi, Current and future trends in polymer membrane-based gas separation technology: A comprehensive review, Journal of Industrial and Engineering Chemistry 98 (2021) 103–129.

[12] R. Castro-Muñoz, V. Martin-Gil, M.Z. Ahmad, V. F\'\ila, Matrimid® 5218 in preparation of membranes for gas separation: Current state-of-the-art, Chem Eng Commun 205 (2018) 161–196.

[13] L.M. Robeson, Correlation of separation factor versus permeability for polymeric membranes, J Memb Sci 62 (1991) 165–185.

[14] L.M. Robeson, The upper bound revisited, J Memb Sci 320 (2008) 390–400.

[15] Y. Xiao, B.T. Low, S.S. Hosseini, T.S. Chung, D.R. Paul, The strategies of molecular architecture and modification of polyimide-based membranes for CO2 removal from natural gas—A review, Prog Polym Sci 34 (2009) 561–580.

[16] R. Swaidan, B. Ghanem, I. Pinnau, Fine-Tuned Intrinsically Ultramicroporous Polymers Redefine the Permeability/Selectivity Upper Bounds of Membrane-Based Air and Hydrogen Separations, ACS Macro Lett 4 (2015) 947–951. https://doi.org/10.1021/acsmacrolett.5b00512.

[17] Y. Wang, X. Ma, B.S. Ghanem, F. Alghunaimi, I. Pinnau, Y. Han, Polymers of intrinsic microporosity for energy-intensive membrane-based gas separations, Mater Today Nano 3 (2018) 69–95.

[18] B. Comesaña-Gándara, J. Chen, C.G. Bezzu, M. Carta, I. Rose, M.-C. Ferrari, E. Esposito, A. Fuoco, J.C. Jansen, N.B. McKeown, Redefining the Robeson upper bounds for CO 2/CH 4 and CO 2/N 2 separations using a series of ultrapermeable benzotriptycene-based polymers of intrinsic microporosity, Energy Environ Sci 12 (2019) 2733–2740.

[19] Z.-X. Low, P.M. Budd, N.B. McKeown, D.A. Patterson, Gas permeation properties, physical aging, and its mitigation in high free volume glassy polymers, Chem Rev 118 (2018) 5871–5911.

[20] T. Corrado, R. Guo, Macromolecular design strategies toward tailoring free volume in glassy polymers for high performance gas separation membranes, Mol Syst Des Eng 5 (2020) 22–48.

[21] C.J. Pedersen, Cyclic polyethers and their complexes with metal salts, J Am Chem Soc 89 (1967) 7017–7036.

[22] D. Wu, C. Yi, Y. Wang, S. Qi, B. Yang, Preparation and gas permeation of crown ether-containing co-polyimide with enhanced CO2 selectivity, J Memb Sci 551 (2018) 191–203.

[23] D. Wu, C. Yi, C.M. Doherty, L. Lin, Z. Xie, A crown ether-containing copolyimide membrane with improved free volume for CO2 separation, Ind Eng Chem Res 58 (2019) 14357–14367.

[24] B. Zhang, J. Qiao, D. Wu, X. He, J. Liu, C. Yi, S. Qi, Enhanced gas separation by free volume tuning in a crown ether-containing polyimide membrane, Sep Purif Technol 293 (2022) 121116.

[25] D. Kim, I. Hossain, A. Husna, T.-H. Kim, Development of CO2-selective polyimide-based gas separation membranes using crown ether and polydimethylsiloxane, Polymers (Basel) 13 (2021) 1927.

[26] D. Wu, X. Qu, X. He, C. Yi, B. Zhang, B. Yang, High-performance carbon molecular sieve membrane derived from a crown ether-containing Co-polyimide precursor for gas separation, Ind Eng Chem Res 62 (2023) 9825–9836.

[27] K. Guo, S. Zhang, K. He, S. Zheng, T. Zhang, T. Yan, Z. Li, Synthesis and characterization of diaminodibenzo-14-crown-4, Chinese Journal of Applied Chemistry 19 (2002) 329–333.

[28] Q. Zhu, X. Ma, H. Pei, J. Li, F. Yan, Z. Cui, H. Wang, J. Li, A highly-efficient lithium adsorptive separation membrane derived from a polyimide-containing dibenzo-14-crown-4 moiety, Sep Purif Technol 247 (2020). https://doi.org/10.1016/j.seppur.2020.116940.

[29] A. van Bondi, van der Waals Volumes and Radii, J Phys Chem 68 (1964) 441–451.

[30] J.Y. Park, D.R. Paul, Correlation and prediction of gas permeability in glassy polymer membrane materials via a modified free volume based group contribution method, J Memb Sci 125 (1997) 23–39.

[31] H. Lin, B.D. Freeman, Permeation and diffusion, Springer Handbook of Materials Measurement Methods (2006) 371–387.

[32] S. Matteucci, Y. Yampolskii, B.D. Freeman, I. Pinnau, Transport of gases and vapors in glassy and rubbery polymers, Materials Science of Membranes for Gas and Vapor Separation (2006) 1–47.

[33] B. Zhang, J. Qiao, D. Wu, X. He, J. Liu, C. Yi, S. Qi, Enhanced gas separation by free volume tuning in a crown ether-containing polyimide membrane, Sep Purif Technol 293 (2022) 121116.

[34] D.R. Rueda, A. Nogales, J.J. Hernández, M.-C. Garc\'\ia-Gutiérrez, T.A. Ezquerra, S. V Roth, M.G. Zolotukhin, R. Serna, Stacking of main chain-crown ether polymers in thin films, Langmuir 23 (2007) 12677–12681.

[35] S. Li, H. McGinness, T. Wang, R. Guo, Crosslinked Matrimid®-like polyimide membranes with unimodal network structure for enhanced stability and gas separation performance, Polymer (Guildf) 237 (2021) 124323.

[36] Y. Zhang, I.H. Musselman, J.P. Ferraris, K.J. Balkus, Gas permeability properties of Matrimid® membranes containing the metal-organic framework Cu–BPY–HFS, J Memb Sci 313 (2008) 170–181. https://doi.org/https://doi.org/10.1016/j.memsci.2008.01.005.

[37] H. Lin, B.D. Freeman, Materials selection guidelines for membranes that remove CO2 from gas mixtures, J Mol Struct 739 (2005) 57–74. https://doi.org/https://doi.org/10.1016/j.molstruc.2004.07.045.

Supporting Information

Tuning Gas Separation Performance of Polyimide Membranes with Macrocyclic Crown Ether Units

Yiwei Su[§], Andrew Seeger[§], Ruilan Guo[*]

Department of Chemical and Biomolecular Engineering, University of Notre Dame, Notre Dame, IN, 46556, USA

***Correspondence:**
Professor Ruilan Guo
rguo@nd.edu
[§] Equal contribution

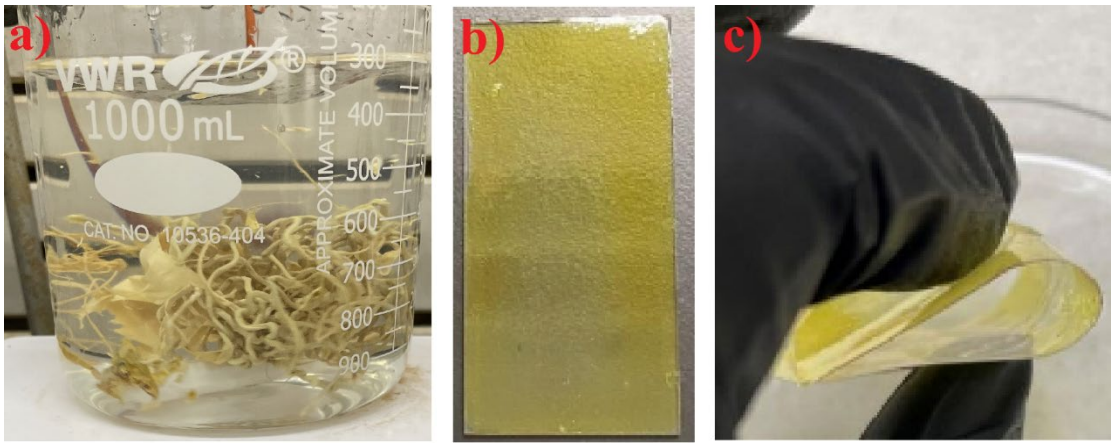

Fig. S1 (a) Fibrous precipitation of MM-DAB18C6(20%) after polycondensation indicating high molecular weight; (b) solution casting of MM-DAB18C6(20%) dense thin film on a glass substrate; (c) formation of robust and flexible MM-DAB18C6(20%) thin film.

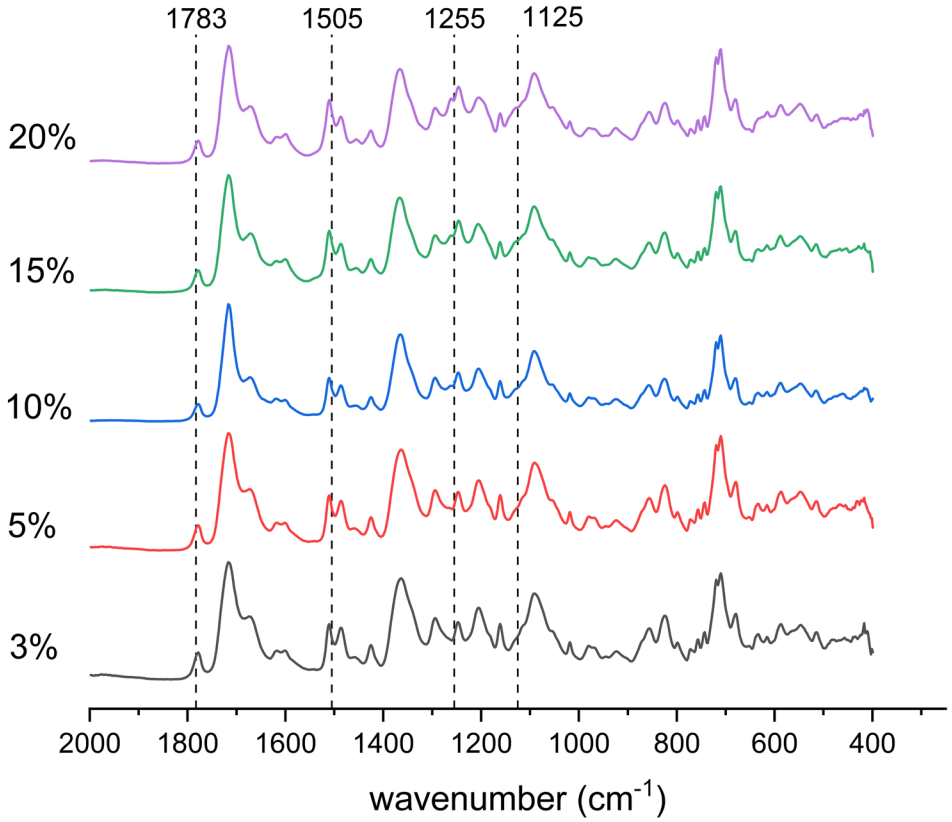

Fig. S2 FTIR spectra of MM-DAB18C6 copolyimides with varying crown ether content. The percentage values are target values.

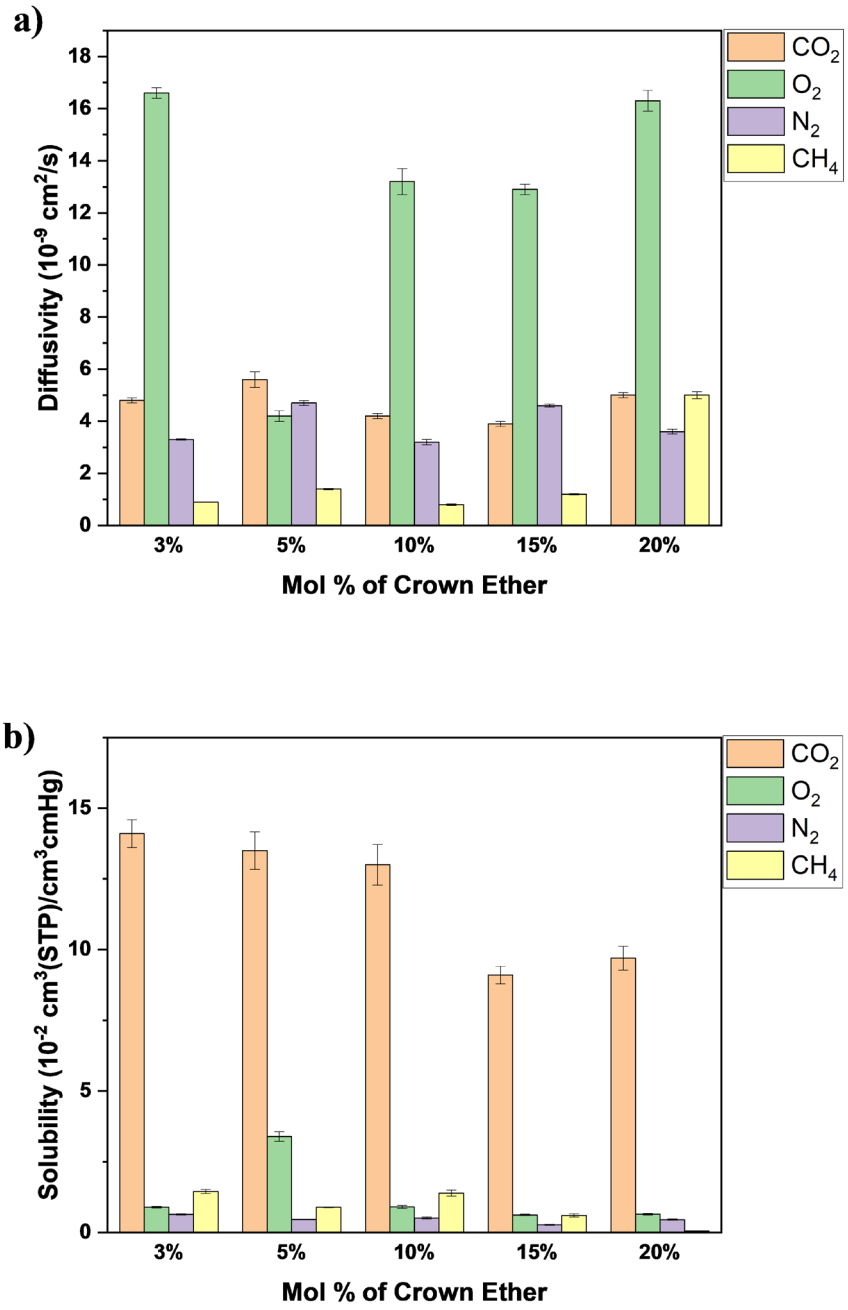

Fig. S3 (a) Diffusivity coefficients and (b) solubility coefficients of MM-DAB18C6 copolyimide films determined via lag-time method and solution-diffusion model.

Table S1 Permeability and ideal selectivity of MM-DAB18C6(x%) copolyimide films

Gas Permeability, *P* (Barrer)					
	H_2	**CO_2**	**O_2**	**N_2**	**CH_4**
Matrimid[1]	17.50	7.29	1.46	0.22	0.21
3% CE	23 ± 0.6	6.95 ± 0.2	1.43 ± 0.04	0.21 ± 0.006	0.14 ± 0.004
5% CE	23.94 ± 0.7	8.26 ± 0.4	1.66 ± 0.09	0.22 ± 0.007	0.15 ± 0.005
10% CE	17.99 ± 0.6	4.8 ± 0.3	1.11 ± 0.03	0.15 ± 0.004	0.11 ± 0.004
15% CE	14.45 ± 1.7	3.32 ± 0.7	0.82 ± 0.1	0.11 ± 0.01	0.07 ± 0.02
20% CE	16.69 ± 0.4	4.74 ± 0.07	1.03 ± 0.02	0.15 ± 0.0007	0.01 ± 0.0007

Ideal selectivity (α)					
	H_2/N_2	**H_2/CH_4**	**CO_2/N_2**	**O_2/N_2**	**CO_2/CH_4**
Matrimid[1]	79.5	83.3	33.1	6.6	34.7
3% CE	109.5	164.3	33.1	6.8	49.6
5% CE	110.8	161.8	38.2	7.7	55.8
10% CE	118.3	168.1	31.6	7.3	44.9
15% CE	129.0	195.3	29.6	7.3	44.8
20% CE	108.4	173.9	30.8	6.7	49.4

[1] Y. Zhang, I.H. Musselman, J.P. Ferraris, K.J. Balkus, Gas permeability properties of Matrimid® membranes containing the metal-organic framework Cu–BPY–HFS, J Memb Sci 313 (2008) 170–181. https://doi.org/10.1016/j.memsci.2008.01.005.

Table S2 Diffusivity and solubility coefficients for MM-DAB18C6(x%) copolyimide films

Diffusivity coefficient (10^{-9} cm^2/s)				
	CO_2	**O_2**	**N_2**	**CH_4**
3% CE	4.82 ± 0.1	16.64 ± 0.2	3.28 ± 0.03	0.90 ± 0.01
5% CE	5.58 ± 0.3	4.17 ± 0.2	4.67 ± 0.1	1.42 ± 0.02
10% CE	4.16 ± 0.1	13.15 ± 0.5	3.2 ± 0.1	0.81 ± 0.03
15% CE	3.90 ± 0.1	12.92 ± 0.2	4.58 ± 0.06	1.17 ± 0.02
20% CE	5.02 ± 0.1	16.34 ± 0.4	3.57 ± 0.1	5.02 ± 0.1

Solubility coefficient (10^{-2} $cm^3(STP)/cm^3cmHg$)				
	CO_2	**O_2**	**N_2**	**CH_4**
3% CE	14.13 ± 0.5	0.89 ± 0.03	0.64 ± 0.03	1.45 ± 0.07
5% CE	13.50 ± 0.7	3.39 ± 0.2	0.46 ± 0.01	0.89 ± 0.02
10% CE	12.98 ± 0.7	0.90 ± 0.05	0.51 ± 0.04	1.39 ± 0.1
15% CE	9.11 ± 0.3	0.62 ± 0.02	0.27 ± 0.02	0.60 ± 0.05
20% CE	9.74 ± 0.4	0.65 ± 0.03	0.45 ± 0.03	0.05 ± 0.006